ASTROPHYSICS OF DENSE QUARK MATTER IN COMPACT STARS*

Armen Sedrakian

Institute for Theoretical Physics, J.W. Goethe-University
60438 Frankfurt am Main, Germany

Massive neutron stars may harbor deconfined quark matter in their cores. I review some recent work on the microphysics and the phenomenology of compact stars with cores made of quark matter. This includes the equilibrium and stability of non-rotating and rapidly rotating stars, gravitational radiation from deformations in their quark cores, neutrino radiation and dichotomy of fast and slow cooling, and pulsar radio-timing anomalies.

1. Introduction

Because of the quark substructure of nucleons predicted by quantum chromodynamics (QCD), nuclear matter will undergo a phase transition to quark matter if squeezed to sufficiently high densities. In the quark matter phase the "liberated" quarks occupy continuum states which, in the low-temperature and high-density regime, arrange themselves in a Fermi sphere. The Fermi-sphere determines the form of low-lying excitation spectrum of quark matter, which resembles that of less exotic low-temperature systems found in condensed matter (*e.g.* electron gas or ultracold atomic vapor) or hadronic physics (*e.g.* nuclear or neutron matter). In analogy to these system the attractive interaction between quarks, mediated by the gluon exchange (which is responsible for the bound state spectrum of QCD, *e.g.*, the nucleon and mesons) leads to quark superconductivity and superfluidity (color superconductivity) via the Bardeen–Cooper–Schrieffer mechanism [1]. Furthermore, under stellar conditions the pairing between the two light flavors of quarks occurs at finite isospin chemical potential, *i.e.*, when the Fermi surfaces of up and down quarks are shifted apart by an amount which is

---

* Talk presented at the EMMI Workshop and XXVI Max Born Symposium "Three Days of Strong Interactions", Wrocław, Poland, July 9–11, 2009.

of the same order of magnitude as the gap in the quasiparticle spectrum. Under these conditions the pairing between the fermions persists, but the actual pairing pattern may be significantly different from that of the BCS and is likely to involve breaking of the spatial symmetries by the condensate order parameter.

During the last decade there has been a substantial progress in understanding of pairing in two-component asymmetric superconductors. Firstly, new developments on (variations of) the Larkin–Ovchinnikov–Fulde–Ferrell (LOFF) phase revealed novel lattice structures of the order parameter [2]. Secondly, it has been suggested that such systems may actually phase separate into normal and superconducting domains [3] or the pairing may require changes in the shapes of the Fermi surfaces [4]. Controlled experiments on two-component cold atomic vapors with mismatched Fermi surfaces show that the phase separation scenario is at work. Whether this is the case in the related systems such as the isospin asymmetric nuclear matter or deconfined quark matter is still unclear. Therefore, a major goal of astrophysics of dense matter is to find and to quantify the manifestations of dense phases in the observable properties of compact stars. Here we review some recent progress towards this goal.

2. Color superconducting phases with broken spatial symmetries

The quark–quark interaction is strongest for pairing between up and down quarks which are antisymmetric in color [1]. At intermediate densities quark matter is composed of up and down quarks, while strange quarks can appear in substantial amounts at higher densities. The leading candidate phase at these densities is the so-called 2SC phase, which is characterized by the order parameter $\Delta \propto \langle \psi^T(x) C \gamma_5 \tau_2 \lambda_2 \psi(x) \rangle$, where τ_2 is the Pauli matrix in the isospin state, λ_2 is the Gell-Mann matrix in the color space, $C = i\gamma^2\gamma^0$ is the matrix of charge conjugation. The isospin chemical potential is determined by the β-equilibrium condition $\mu_d - \mu_u = \mu_e \sim 100\,\text{MeV}$ among d and u quarks and electrons, where μ_i with $i = d, u, e$ are the chemical potentials. The Fermi spheres of up and down quarks are shifted apart by this amount. Thus, the cross-flavor pairing must overcome the disruptive effect of mismatched Fermi surfaces. Furthermore, if the physical strange quark mass is close to its current mass $\sim 100\,\text{MeV}$, electrons may be gradually replaced by strange quarks, which again will disfavor the cross-flavor pairing.

A superconducting phase with asymmetric cross-species pairing needs to optimize the overlap between the Fermi surfaces (which is perfect in the symmetric BCS state) to attain the maximum possible condensation energy. There are a number of ways to achieve this: *(a)* condensate that carries non-

zero momentum with respect to some fixed frame. The penalty in the energy budget for the (always positive) kinetic energy of condensate motion is compensated by the gain in the (negative) condensation energy. In three-flavor quark matter the face-centered cubic (fcc) lattices were identified as having particularly low free energy [2] in the regime where the Ginzburg–Landau (GL) theory is applicable. The spatial form of the condensate beyond the GL regime is not known, therefore current treatments beyond this regime require some simplifying assumptions [5, 6]. *(b)* A more symmetric superconducting phase exploits deformations of Fermi spheres as the mechanism of restoring the coherence needed for pairing at the cost of kinetic energy loss caused by these deformations. The deformed Fermi surface phase requires minimal breaking of spatial symmetry and is more symmetric than the lattice phases above [4].

In this review we will be concerned mainly with the 2SC and the crystalline color superconducting (CCS) phases. We expect that the phenomenology of related phases with cross-flavor pairing is essentially the same.

3. Equilibrium and stability

The central question, which we address in this section, is whether the equation of state of matter at high densities admits stable configurations of self-gravitating objects in General Relativity featuring deconfined quark matter. The deconfinement phase transition from baryonic to quark matter leads to a softening of the equation of state which could lead to an instability towards a collapse into a black hole. In Ref. [7] the quark phase was studied in the Nambu–Jona-Lasinio (NJL) model, which is a low-energy nonperturbative approximation to QCD, that is anchored in the low-energy phenomenology of the hadronic spectrum. While dynamical symmetry breaking, by which quarks acquire mass, is incorporated in this model, it lacks confinement. Physically, the true nuclear equation state must go over to some sort of quark equation of state at some density if the deconfinement has to take place in nature. If pressure *versus* chemical potential curves for chosen equations of state of nuclear and quark matter do not cross, then the models are incompatible in the sense that they cannot describe the desired transition between the nuclear and quark matter. The low-density equation of state of nuclear matter and the high-density equation of state of CCS matter were matched in Ref. [7] at an interface via the Maxwell construction. The phase with largest pressure is the one that is realized at a given chemical potential. Thus, at the deconfinement phase transition there is a jump in the density at constant pressure as illustrated in Fig. 1, left panel. The low-density nuclear equations of state are based on the Dirac–Bruckner–Hartree–Fock approach and are the most hard equations of state in our collection [8, 9]. It should

be noted that the matching with softer equations of state can be enforced by varying the normalization of the pressure ("effective bag constant") of the quark matter, in which case the density of deconfinement is a free parameter.
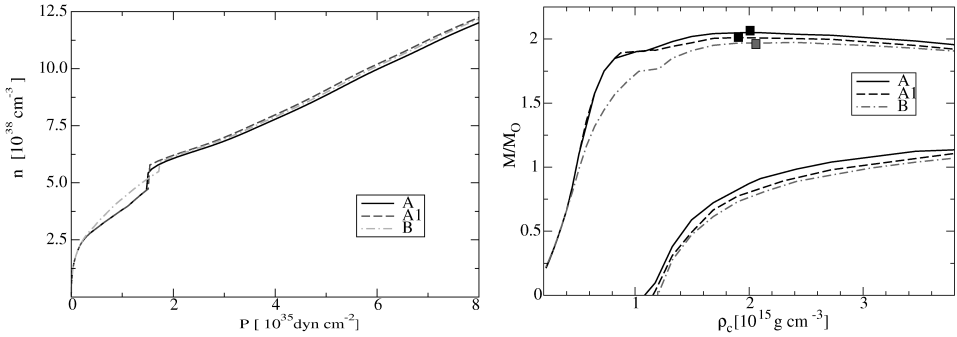

Fig. 1. Left panel: Number density *versus* pressure for three models. For the models A and A1 the nuclear (low density) equation of state is the same; for the models A and B the quark (high density) equation of state is the same. Right panel: Dependence of the total stellar mass and the mass of the quark core in units of solar mass $M_\odot$ on the central density for non-rotating configurations. The lower set of curves represents the masses of the CCS quark cores, the upper set — the total masses of the configurations. The maximal masses are marked with boxes.

The spherically symmetric solutions of Einstein's equations for self-gravitating fluids are given by the well-known Tolman–Oppenheimer–Volkoff equations [8]. A generic feature of these solutions is the existence of a maximum mass for any equation of state; as the central density is increased beyond the value corresponding to the maximum mass, the stars become unstable towards collapse to a black hole. A criterion for the stability of a sequence of configurations is the requirement that the derivative $dM/d\rho_c$ should be positive (the mass should be an increasing function of the central density).

For configurations constructed from a purely nuclear equation of state the stable sequence extends up to a maximum mass of the order of 2 $M_\odot$ (Fig. 1), this large value being a consequence of hardness of the equation of state. The hybrid configurations branch off from the nuclear configurations when the central density reaches that of the deconfinement phase transition. It is seen that a stable branch of hybrid stars emerges in the range of central densities $1.3 \leq \rho_c \leq 2.5 \times 10^{15}$ g cm^{-3}. The masses of the CCS quark cores cover the range $0 \leq M_{\text{core}}/M_\odot \leq 0.75 - 0.88$ for central densities $1.3 \times 10^{15} \leq \rho_c \leq 2 \times 10^{15}$. Thus, the quark core mass ranges from one third to about the half of the total stellar mass.

Millisecond neutron stars can rotate at frequencies which are close to the limiting orbital Keplerian frequency at which mass shedding from the equatorial plane starts. The Keplerian frequency sets an upper limit on the rotation frequency, since other (less certain) mechanisms, such as secular instabilities, could impose lower limits on the rotation frequency. The mass *versus* central density dependence of compact stars rotating at the Keplerian frequency is similar to that for non-rotating stars with the scales for mass shifted to larger values [7]. The increase in the maximum mass for stable hybrid configurations (in solar mass units) is $2.052 \rightarrow 2.462$ for the model A, $2.017 \rightarrow 2.428$ and 2.4174 for the model A1 (there are two maxima) and $1.981 \rightarrow 2.35$ for the model B [7].

Thus, a new branch of *stable hybrid configurations* with CCS matter cores emerges within a broad range of central densities. The quark equation of state depends only on the NJL model parameters (*i.e.* does not contain an additional "bag constant"). A quite general conclusion of our analysis is that the nuclear equation of state needs to be *hard* to enable thermodynamical equilibrium with the NJL model quark matter.

4. Gravitational radiation

Continuous gravitational waves emitted by non-axisymmetric rotating compact stars are expected to be in the bandwidth of current gravitational wave interferometric detectors. Upper limits on the strain of gravitational waves from a selection of radio pulsars were set by the LIGO Collaboration [10]. Gravity waves arise from time-dependent quadrupole deformations of masses. Therefore, rotating isolated neutron stars will emit gravitational radiation if their mass distribution is non-axisymmetric with respect to their rotation axis. The axial symmetry of the star's core can be broken by the solid deformations in CCS matter, whose shear modulus μ_{shear} was computed in Ref. [11]. Initially, the gravitational wave emission from a quark star made of uniform-density incompressible CCS matter was estimated by Lin [12]. Haskell *et al.* [12] estimated core deformations and associated with them constraints on the QCD parameters for sequences of 1.4 $M_\odot$ and $R = 10$ km stars composed of CCS incompressible quark cores and hadronic shells obeying $n = 1$ polytropic equation of state. Gravitational radiation of models based on realistic equations of state were considered in Ref. [13]. One key difference to the previous models is that realistic hybrid configurations have masses that are close to the maximum sustainable mass $M_{\text{max}} \simeq 2M_\odot$. Furthermore, the quadrupole moment of the quark core was computed from realistic density profile, which differs substantially from constant density profile of an incompressible fluid, see Fig. 2. The characteristic strain amplitude of gravitational waves emitted by a triaxial star rotating about its
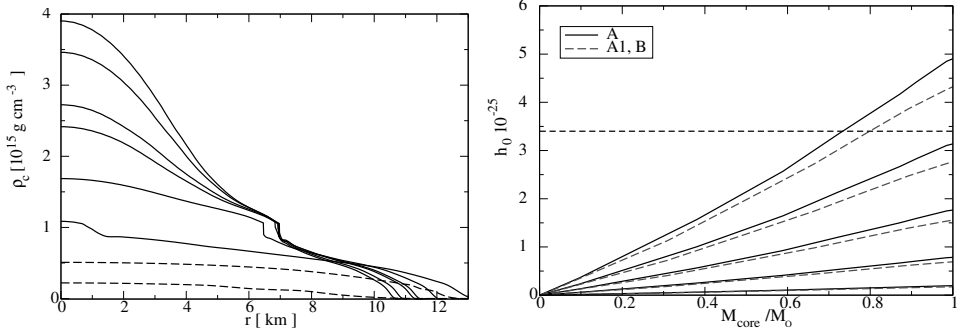
Fig. 2. Left panel: dependence of density on the internal radius (model A). The dashed lines correspond to purely nuclear, the solid lines — to hybrid configurations. Density jumps at the phase transition to quark matter. Right panel: the strain of gravitational wave emission of the Crab pulsar. Each triple of curves corresponds to the gap value (from top to bottom) $\Delta = 50, 40, 30, 20$, and 10 MeV and the breaking strain $\bar{\sigma}_{\max} = 10^{-4}$. The horizontal line shows the current experimental upper limit.

principal axis is $h_0 = 16\pi^2 G c^{-4} \varepsilon I_{zz} \nu^2 r^{-1}$, where ν is the star's rotation frequency, r is the distance to the observer, $\varepsilon = (I_{xx} - I_{yy})/I_{zz}$ is the equatorial ellipticity, I_{ij} is the tensor of moment of inertia, G is the gravitational constant, c is the speed of light. The elastic deformations are assumed to be small perturbation on the background equilibrium of the star. Fig. 2 displays the strain of gravitational wave emission as a function of the core mass M_{core} and the current upper limit for the Crab pulsar $h_0 < 3.4 \times 10^{-25}$, which is rotating at the frequency $\nu = 29.6$ Hz at the distance 2 kpc [10]. The value of the breaking strain of CCS core is $\bar{\sigma}_{\max} = 10^{-4}$. The dependence of the stain amplitude on the microscopic parameters follows from the chain $h_0 \propto Q_{\max} \propto \mu_{\mathrm{shear}} \propto \bar{\sigma}_{\max} \Delta^2$, whereby $Q_{\max}$ is the maximal quadrupole moment of the CCS core. The strain of gravitational wave emission is close to the upper limit for $\Delta = 50$ MeV. If, however, the gaps are small more "optimistic" values of $10^{-3} \leq \bar{\sigma}_{\max} \leq 10^{-2}$ will be needed to generate sizeable strain amplitude. The Crab puslar's current limit implies $\bar{\sigma}_{\max} \Delta^2 \sim 0.25$ MeV^2, assuming maximally strained matter. The evolutionary avenues that may lead to such maximal deformations are not known. Pulsars may simply preserve their initial deformations as they cool down and solidify in the CCS state. We conclude that *massive compact stars with CCS quark cores are strong candidate sources of gravitational wave emission.* Improved upper limits on the strain amplitude, can narrow down the admissible range of parameters of the CCS matter in the future.

5. Neutrino emission and cooling

Neutrino emissivities control the cooling rate of a neutron star during the first $10^4 - 10^5$ yr of their evolution. At later times the photon emission from the surface and the heating in the interior are the main factors. Depending on the dominant neutrino emission process in the neutrino emission era $t \leq 10^5$ yr the cooling could be slow (standard) or fast (nonstandard).

The slow cooling scenario is based on neutrino cooling via the modified Urca and bremsstrahlung processes. The fast cooling requires unconventional processes such as decays in pion/kaon condensates, direct Urca process on nucleons, hyperons, or quarks. Phase-space arguments show that fast cooling neutrino processes have typically temperature dependences $\sim T^6$, whereas those leading to slow cooling require additional phase space for the spectator particle and their emissivities scale as T^8.

An inspection of the observational data on neutron star surface temperatures, which is commonly presented on a plot of photon-luminosity (or surface temperature) *versus* age, shows that the data cannot be described by a single cooling track; a regulator is needed that will cool some stars faster than the others [8,9]. It is reasonable to assume that the heavier stars cool via some fast mechanism, while the lighter stars cool slowly via the modified processes. Indeed, the fast cooling agents operate above a certain density threshold. Therefore, the dichotomy of observed high and low surface temperature could be an evidence of a fast process operating in massive stars. Thus, we are led to examine the potential fast cooling processes in the quark cores of compact stars. The key process is the Urca processes (quark β-decay) $d \rightarrow u + e + \bar{\nu}_e$ and $u + e \rightarrow d + \nu_e$, which is permitted in *interacting* quark matter for any asymmetry between u and d quarks. The effect of asymmetric pairing is well demonstrated on the example of 2SC phase [14,15]. The result for the emissivity depends on whether the parameter $z = \Delta/\delta\mu$ is larger or smaller than unity, where Δ is the gap in the 2SC phase and $\delta\mu = \mu_d - \mu_u$ is the shift in the chemical potentials of the up and down quarks. For $z > 1$ all the particle modes are "gapped", therefore, as the temperature is lowered, the emissivity is suppressed (for asymptotically low temperatures exponentially). When $z < 1$ there are gapless modes in the quasiparticle spectrum; this implies that the neutrino production is not affected by color superconductivity. As a result, the superconducting quark matter cools at a rate comparable to the unpaired matter. More generally, we may conclude that *the existence of ungaped segments on the Fermi surfaces of quarks will lead to an enhanced cooling of these stars.* A density dependent z parameter may resolve the dichotomy of the fast and slow cooling by providing a smooth transition between these extremes.

6. Radio-timing and rotational anomalies

Pulsars are nearly prefect clocks, whose pulsed emissions, with a typical periodicity of seconds or less, are locked to the rotation period of the star. Their periods increase gradually over time, due to a secular loss of rotational energy. Some pulsars show deviations from this regularity. The pulsar timing anomalies divide roughly into three types. *(i) Glitches.* These are distinguished by abrupt increases in the rotation and spin-down rates of pulsars by amounts $\Delta\Omega/\Omega \sim 10^{-6}$–$10^{-8}$ and $\Delta\dot{\Omega}/\Omega \sim 10^{-3}$. After a glitch, $\Delta\Omega/\Omega$ and $\Delta\dot{\Omega}/\Omega$ slowly relax toward their pre-glitch values, on a time scale of order weeks to years, in some cases with permanent hysteresis effects. Such behavior is attributed to a component within the star that is only weakly coupled to the rigidly rotating normal component responsible for the emission of pulsed radiation. *(ii) Timing Noise.* These represent irregular, stochastic deviations in the spin and spin-down rates that are superimposed on the near-perfect periodic rotation of the star. Whether the superfluids are involved in the generation of timing noise remains unclear. *(iii) Long-Term Periodic Variabilities.* Observed in the timing of few pulsars, most notably PSR B1828-11, these deviations strongly constrain theories of superfluid friction, if their periodicities are interpreted in terms of precession. (Note however that the Tkachenko modes of the vortex lattice are a viable alternative to the precession interpretation [17].) The importance of the inferred precession mode stems from the fact that it involves non-axisymmetric perturbations of the rotational state, removing the degeneracy with respect to ζ ($\zeta' \simeq 0$) that is inherent in the interpretation of post-glitch dynamics.

The macroscopic physics of neutron-star rotation and its anomalies observed in the timing of pulsars can be described within the hydrodynamic theory of superfluids. At the local hydrodynamical scale, the rate of angular momentum transfer between the superfluid and normal components is determined by the equation of motion of a vortex line in a neutral superfluid

$$\omega_{\mathrm{S}}(\boldsymbol{v}_{\mathrm{S}} - \boldsymbol{v}_{\mathrm{L}}) \times \boldsymbol{\nu} + \zeta(\boldsymbol{v}_{\mathrm{L}} - \boldsymbol{v}_{\mathrm{N}}) + \zeta'(\boldsymbol{v}_{\mathrm{L}} - \boldsymbol{v}_{\mathrm{N}}) \times \boldsymbol{\nu} = 0 \,, \tag{1}$$

where $\boldsymbol{v}_{\mathrm{S}}$ and $\boldsymbol{v}_{\mathrm{N}}$ are the superfluid and normal fluid velocities, $\boldsymbol{v}_{\mathrm{L}}$ is the velocity of the vortex, $\boldsymbol{\nu}$ is a unit vector along the vortex line, ω_{S} is the unit of circulation, and ζ, ζ' are (dimensionless) friction coefficients, also known as the drag-to-lift ratios. These coefficients encode the essential information on the microscopic processes of interaction of vortices with the ambient unpaired fluid.

The potential role of quark matter in the rotational dynamics of compact stars is not understood yet. Some of the candidate phases, such as the color-flavor-locked (CFL) phase, rotate by creating vortices [18], which interact with the phonon gas within this phase [19]. However, phonons do

not interact electromagnetically with the rest of the star, therefore it is unclear on which timescales the CFL quark core will couple to the observable crust. Such a coupling is manifest for the 2SC and related phases, where the magnetic field (partially) penetrates into the superfluid region. While the vortices in these phases (if any) are not rotational in nature, their electromagnetic coupling to the vortices in the hadronic core and to electrons, which are shared with less denser phases of the star, can impact the rotational dynamics of pulsars.

REFERENCES

[1] D. Bailin, A. Love, *Phys. Rep.* **107**, 325 (1984); M. Alford, K. Rajagopal, in *Pairing in Fermionic Systems*, Eds. A. Sedrakian, J.W. Clark, M. Alford, World Scientific, Singapore 2006, p. 1, `arXiv:hep-ph/0606157`; S.B. Rüster, V. Werth, M. Buballa, I.A. Shovkovy, D.H. Rischke, *ibid.*, p. 63 `arXiv:nucl-th/0602018`; T. Schafer, *ibid.*, p. 109, `arXiv:nucl-th/0602067`; M.G. Alford, `arXiv:0907.0200[nucl-th]`.

[2] J.A. Bowers, K. Rajagopal, *Phys. Rev.* **D66**, 065002 (2002) `[arXiv:hep-ph/0204079]`; K. Rajagopal, R. Sharma, *Phys. Rev.* **D74**, 094019 (2006) `[arXiv:hep-ph/0605316]`; *J. Phys. G* **32**, S483 (2006) `[arXiv:hep-ph/0606066]`; N.D. Ippolito, G. Nardulli, M. Ruggieri, *J. High Energy Phys.* **0704**, 036 (2007) `[arXiv:hep-ph/0701113]`.

[3] P.F. Bedaque, H. Caldas, G. Rupak, *Phys. Rev. Lett.* **91**, 247002 (2003); H. Caldas, *Phys. Rev.* **A69**, 063602 (2004).

[4] H. Müther, A. Sedrakian, *Phys. Rev. Lett.* **88**, 252503 (2002) `[arXiv:cond-mat/0202409]`; *Phys. Rev.* **C67**, 015802 (2003) `[arXiv:nucl-th/0209061]`; *Phys. Rev.* **D67**, 085024 (2003) `[arXiv:hep-ph/0212317]`; A. Sedrakian, in *Superdense QCD Matter and Compact Stars*, Eds. D. Blaschke and D. Sedrakian, Springer, Dordrecht 2006, p. 209 `[arXiv:nucl-th/0312053]`.

[5] D. Nickel, M. Buballa, *Phys. Rev.* **D79**, 054009 (2009) `[arXiv:0811.2400[hep-ph]]`.

[6] A. Sedrakian, D.H. Rischke, *Phys. Rev.* **D80**, 074022 (2009) `[arXiv:0907.1260[nucl-th]]`.

[7] N. Ippolito, M. Ruggieri, D.H. Rischke, A. Sedrakian, F. Weber, *Phys. Rev.* **D77**, 023004 (2008) `[arXiv:0710.3874[astro-ph]]`.

[8] F. Weber, *Pulsars as Astrophysical Laboratories for Nuclear and Particle Physics*, Bristol, U.K.: Institute of Physics, 1999.

[9] A. Sedrakian, *Prog. Part. Nucl. Phys.* **58**, 168 (2007)
    `[arXiv:nucl-th/0601086]`.

[10] B. Abbott *et al.* [LIGO Scientific Collaboration], *Astrophys. J. Lett.* **683**, 45
    (2008).

[11] M. Mannarelli, K. Rajagopal, R. Sharma, *Prog. Theor. Phys. Suppl.* **174**, 39
    (2008).

[12] L.-M. Lin, *Phys. Rev.* **D76**, 081502(R) (2007); B. Haskell, N. Andersson,
    D.I. Jones, L. Samuelsson, *Phys. Rev. Lett.* **99**, 231101 (2007).

[13] B. Knippel, A. Sedrakian, *Phys. Rev.* **D79**, 083007 (2009) `[arXiv:0901.4637`
    `[astro-ph.SR]]`.

[14] M. Alford, P. Jotwani, C. Kouvaris, J. Kundu, K. Rajagopal, *Phys. Rev.* **D71**,
    114011 (2005) `[arXiv:astro-ph/0411560]`; R. Anglani, G. Nardulli,
    M. Ruggieri, M. Mannarelli, *Phys. Rev.* **D74**, 074005 (2006)
    `[arXiv:hep-ph/0607341]`.

[15] P. Jaikumar, C.D. Roberts, A. Sedrakian, *Phys. Rev.* **C73**, 042801(R) (2006)
    `[arXiv:nucl-th/0509093]`.

[16] A. Sedrakian, I. Wasserman, J.M. Cordes, *Astrophys. J.* **524**, 341 (1999)
    `[arXiv:astro-ph/9801188]`; B. Link, *Astrophys. Space Sci.* **308**, 435 (2007);
    T. Akgun, B. Link, I. Wasserman, *Mon. Not. R. Astron. Soc.* **365**, 653 (2006)
    `[arXiv:astro-ph/0506606]`; B. Link, `arXiv:astro-ph/0608319`.

[17] J. Noronha, A. Sedrakian, *Phys. Rev.* **D77**, 023008 (2008) `[arXiv:0708.2876`
    `[astro-ph]]`.

[18] K. Iida, G. Baym, *Phys. Rev.* **D66**, 014015 (2002).

[19] M. Mannarelli, C. Manuel, B.A. Sa'd, *Phys. Rev. Lett.* **101**, 241101 (2008)
    `[arXiv:0807.3264 [hep-ph]]`.